Journal of Cranio-Maxillo-Facial Surgery 47 (2019) 1475–1483

Contents lists available at ScienceDirect

Journal of Cranio-Maxillo-Facial Surgery

journal homepage: www.jcmfs.com

The evolution of craniofacial resection: A new workflow for virtual planning in complex craniofacial procedures

Alessandro Tel [a], Daniele Bagatto [b], Francesco Tuniz [c], Salvatore Sembronio [a], Fabio Costa [a], Serena D'Agostini [b], Massimo Robiony [a, *]

[a] Maxillofacial Surgery Department, Academic Hospital of Udine, Department of Medicine, University of Udine, Italy
[b] Neuroradiology Department, Academic Hospital of Udine, Department of Medicine, University of Udine, Italy
[c] Neurosurgery Department, Academic Hospital of Udine, Department of Medicine, University of Udine, Italy

ARTICLE INFO

Article history:
Paper received 2 February 2019
Accepted 27 June 2019
Available online 3 July 2019

Keywords:
Virtual surgical planning
Accuracy
Craniofacial
Computer-guided surgery
Navigation
Facial care project

ABSTRACT

Complex craniofacial surgery has been later to take advantage of computerized planning than traditional maxillofacial procedures. Virtual reality, 3D model navigation, and bioengineering analyses have changed our approach to the surgical planning of craniofacial resection, increasing the benefits of surgery in terms of accuracy while decreasing complication rate.

This study introduces a new workflow for 3D reconstruction, virtual model navigation, and alignment analyses, and demonstrates its successful application in a sample of four patients. A case of squamous cell carcinoma of the maxillary and ethmoid sinus in a 62-year-old patient is presented to evaluate the application of the workflow for a combined transfacial and transcranial resection. Results demonstrate that virtual surgical planning was successfully translated into navigational coordinates and reproduced in the operating room.

While the literature provides a wide range of applications of virtual planning for traditional maxillofacial procedures, its introduction for complex craniofacial procedures remains difficult. The presented case shows that it is worth investigating the correlation between virtual reality planning and surgical accuracy for craniofacial resection, and related advantages in terms of surgical safety and improved prognosis.

1. Introduction

Malignant tumors of the nasal cavity and paranasal sinuses are infrequent, accounting for less than 3% of upper aerodigestive tract cancers and representing 0.2–0.5% of all cancer cases. 80% of these tumors are diagnosed in people aged 45–85 years, and men are affected 1.5 times more than women (Robin et al., 1979).

A wide variety of tumors occur in the nose or paranasal sinus, such as cancers of endodermal, mesodermal, and epidermal origins. These include squamous cell carcinoma, melanoma, lymphoma, sarcoma, hemangiopericytoma, malignant giant cell tumor, basal cell carcinoma, plasmacytoma, adenoid cystic carcinoma, mucoepidermoid carcinoma, malignant meningioma, and metastatic malignancies. Squamous cell carcinoma, sinonasal undifferentiated carcinoma (SNUC), and adenocarcinoma represent the most common histological types. Adenoid-cystic carcinoma accounts for fewer of cases, while mucoepidermoid, acinic cell carcinomas and sarcomas are uncommon. A rare but typical tumour of this region is esthesioneuroblastoma.

The most frequent localization of sinonasal malignancies is the maxillary sinus (60–70%), followed by the nasal cavity itself (20–30%). It is estimated that 10–15% of cases occur in the ethmoid air cells, while frontal and sphenoid sinuses account for the remainder of neoplasms (Bridger et al., 1991; Turner and Reh, 2012). Advanced tumours of the skin of the face or scalp might present with anterior skull base involvement. Similarly, tumours of the orbit and/or maxillary sinus might present with ethmoidal extension in advanced stages (Cantù et al., 2006).

Sinonasal malignancies can grow to a considerable size before patients develop any concerns. Initial symptoms can be mild and include nasal fullness, nose bleeding, and smell disorder, which mimic common sinonasal diseases and can therefore lower suspicion of apparently serious disease. As a consequence, presentation

* Corresponding author. P.le S. Maria della Misericordia 1, 33100 Udine, Italy.
E-mail address: massimo.robiony@uniud.it (M. Robiony).

https://doi.org/10.1016/j.jcms.2019.06.016
1010-5182/

is generally late, while surgical resection can be extensive and carry a high risk due to the involvement of critical anterior cranial base structures (Taghi et al., 2012).

Many therapeutic approaches have been proposed for carcinoma of the nasal cavity and paranasal sinuses. Although endoscopic surgery has been applied to some extent in sinonasal malignancies in selected cases, and some studies have reported comparable results in terms of overall survival (Eloy et al., 2009; Batra et al., 2010), complete surgical resection remains the method of choice for advanced disease (Dulguerov et al., 2001). Additionally, the best outcomes have been reported when surgery was followed by postoperative adjuvant radiotherapy (Blanco et al., 2004; Hoppe et al., 2007), with an increase in 5-year disease-free survival rates to at least 50% for specific histotypes (e.g. adenocarcinomas and esthesioneuroblastomas) and 5-year survival rates of up to 70–80% versus 25% when subtotal tumor resection was followed by adjuvant radiation therapy (Vrionis et al., 2004).

En bloc craniofacial resection has been widely recognized as the treatment of choice for malignancies approaching or involving the cribriform plate. In recent decades, several techniques have been described and four variants can be acknowledged: the classic double transcranial and transfacial approach; a transcranial approach only; a transfacial approach only; and a subcranial approach avoiding any facial incision.

Accurate planning in such anatomical regions is associated with a lower complication rate and improved prognosis; however, due to limited visibility and a narrow surgical field that is easily filled with blood, precision is difficult to achieve, and surgical maneuvers are limited.

Modern software offers the possibility to create accurate anatomical models and has allowed new approaches to planning surgical procedures. Digital models based on high-resolution polygonal meshes provide surgeons with the opportunity to design osteotomies preoperatively, simulate skeletal movements, and visualize operative options in multistage approaches, such as complex craniofacial procedures (Day et al., 2018; Guo et al., 2018). Moreover, surgical navigation represents a bridge between virtual planning and the real patient (Wang et al., 2015). However, relatively little evidence is found in the literature concerning the application of virtual surgical planning in complex surgical procedures requiring a double transcranial and transfacial approach.

The purpose of this study was to modernize the management of surgical planning for craniofacial resections by introducing the following innovations:

- Improving the creation of virtual models through segmentation of merged TC and MRI datasets.
- Detailed virtual surgical planning, representing the whole sequence of osteotomies for dismantling and reconstructing the craniofacial skeleton, according to oncological principles.
- Navigating detailed virtual surgical plans, including accurate tumor models and three-dimensional osteotomies, instead of basic imaging or simple navigator-generated plans.
- Providing a three-dimensional evaluation of surgical accuracy using qualitative and quantitative parameters.

1.1. Technical report

This study presents a new workflow, combining virtual surgical planning and navigation, in four patients with advanced paranasal sinus neoplasms and cranial base involvement, who underwent anterior or antero-lateral craniofacial resection in 2017–18 (Table 1). Technical aspects are analyzed and one case is presented in detail to demonstrate the application of the workflow.

1.1.1. Improving digital models of patients and disease

In order to achieve the most accurate 3D-reconstruction it is of utmost importance to acquire the appropriate imaging. All patients involved in this study underwent both standard preoperative CT and MR examination. All MR examinations were performed on a 1.5-T scanner (Aera; Siemens, Erlangen, Germany) before and after contrast media (CM) administration (Gadovist; Schering Bayer Pharma, Leverkusen, Germany) at a dose of 0.1 mmol/kg of body weight (as indicated by the manufacturer). The MR acquisition protocol included non-enhanced axial and coronal turbo spin echo (TSE) T2W sequences, axial spin echo (SE) T1W sequences with and without fat suppression, axial diffusion-weighted imaging (DWI), and enhanced VIBE-T1W, 3D-T2, and 3D-T1 weighted sequences.

All CT examinations were performed without CM injection from the vertex capitis to the lower margin of the mandible on a 64-row scanner (LightSpeed VCT 64; General Electric, Milwaukee, USA). The main technical parameters for CT were the following: 100 kV; 120 mA; row thickness = 0.625; noise index = 7; rotation time = 1.0 s. In order to achieve a unique image containing the most relevant information from the two different techniques, digital imaging and communication in medicine (DICOM) datasets of 3D-T1-weighted sequences (TR = 1400 ms; TE = 3.5 ms; slice thickness = 1.0 mm; number of slices = 240; FOV = 223 × 255; flip angle = 15°) and CT acquisitions were coregistered and merged. It was therefore possible to obtain optimal definition of bony structures together with pathological soft tissue enhancement of the different lesions. In all cases, a postoperative CT examination was also performed before discharge in order to exclude surgical complications.

DICOM files of CT and MRI sequences were transferred to Mimics software (Materialise, Leuven, Belgium) and coregistered to perform multimodality image segmentation. All images were reoriented within the same coordinate system and merged into a common volume for segmentation of different structures (Fig. 1A, B).

First the skull was segmented by applying a thresholding algorithm. Using a combination of semi-automated and manual methods, the tumor was segmented by two independent operators (AT and DB). Using regional growing algorithms and manual refinement, the internal carotid artery was localized and segmented. The optical nerve was manually traced on the MRI scan. Masks resulting from segmentation of individual structures were then converted into polygonal meshes with no smoothing algorithm applied, in order to preserve the highest anatomical correspondence.

1.1.2. Detailed virtual surgical planning: representing the surgical sequence

After 3D-models were created, virtual surgical planning was performed on the skull in ProPlan CMF (Depuy Synthes, Solothurn, Switzerland and Materialise, Leuven, Belgium) and osteotomies were simulated to access the tumor according to the combined craniofacial approach.

Based on a color map computing the spatial differences between tumor and bone, osteotomies were virtually traced with a safety margin of at least 5 mm. Osteotomies were created in the following order: 1) bifrontal craniotomy, 2) anterior cranial fossa osteotomy, 3) lateral rhinotomy, 4) right maxillectomy. The following bone segments were designed: frontal bone flap, right orbital and ethmoidal roof, nasal bones, right maxilla. In particular, the right orbito-ethmoidal roof and right maxilla segments represented the limits for tumor box-resection.

1.1.3. Navigating detailed virtual surgical plans

Skull, bone segments, and tumor model were individually exported as STL files and imported into navigation software (iPlan 3.0; BrainLab, Feldkirchen, Germany), where models were aligned

Table 1
Demographic, clinical, surgical, and technological characteristics of the sample of patients undergoing the protocol for virtual 3D reconstruction and evaluation of accuracy in craniofacial resection. The case report section describes case 2.

No.	Age	Sex	Year	Lesion	Local extension	Application of the new protocol	Surgical approach	Reconstruction	Surgical navigation	Imaging and planning	Accuracy measurement
1	66	M	2017	Sinonasal undifferentiated carcinoma	T3	Yes	Combined transfacial and transcranial	Anterolateral thigh flap	Yes (navigation of VSP)	Hybrid CT + MRI 3D virtual planning	3D part comparison analysis
2	62	M	2017	Squamous cell carcinoma	T4a	Yes	Combined transfacial and transcranial	Latissimus dorsi flap	Yes (navigation of VSP)	Hybrid CT + MRI 3D virtual planning	3D part comparison analysis
3	49	M	2018	Adenocarcioma	T4a	Yes	Combined transfacial and transcranial	Latissimus dorsi flap	Yes (navigation of VSP)	Hybrid CT + MRI 3D virtual planning	3D part comparison analysis
4	50	M	2018	Squamous cell carcinoma	T4a	Yes	Combined transfacial and transcranial	Anterolateral thigh flap	Yes (navigation of VSP)	Hybrid CT + MRI 3D virtual planning	3D part comparison analysis

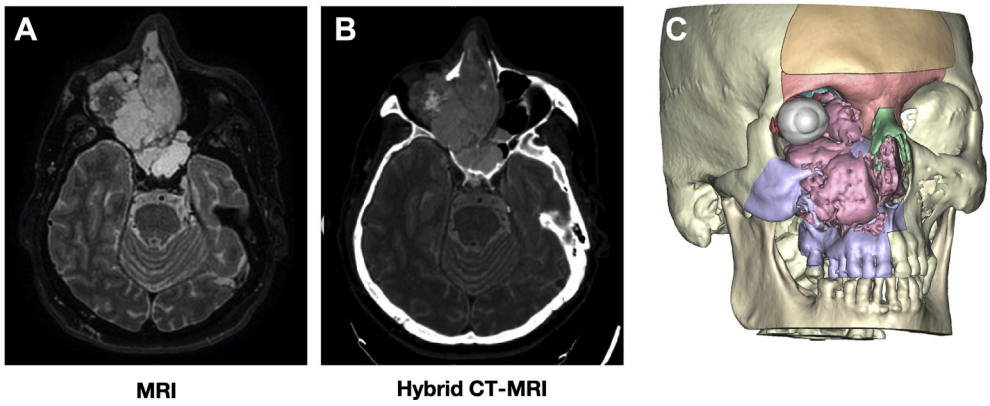

Fig. 1. Image registration process and virtual 3D model reconstruction. A) The 3D-T1 weighted MR sequence is suitable for identifying the tumor mass, but bone tissue is poorly visible. B) Coregistered 3D-T1 weighted MR and CT scans are merged in a single DICOM dataset, including soft-tissue definition from MR and bone contrast from CT. C) The combined dataset is segmented and polygonal meshes of anatomical structures are created. Osteotomies are designed and the surgical plan is established on virtual models.

to the DICOM dataset that was used for navigation. Then the project was imported into the Brainlab surgical navigator to navigate the surgical planning performed in ProPlan CMF and to allow replication of virtual osteotomies in the real patient (Fig. 2).

Before surgery, an optical tracking system was installed, consisting of a stereoscopic infrared camera and a dynamic reference frame (DRF) represented by a mini tripod skull-reference system, which was fixed onto the cranial vault using a self-drilling screw. DRF allowed for head motion and patient repositioning, which are necessary during complex craniofacial surgeries. In order to match coordinate systems of the real patient space and the virtual image space, image-to-patient registration was performed using a point pair matching algorithm based on anatomical landmarks (canthi, nasion, nose tip, and supraorbital rims), as indicated by the navigation software. Although slightly less accurate than fiducial markers-based registration, anatomical landmarks are proven to provide sufficient accuracy for many procedures concerning frontally located targets (Willems et al., 2001). Most importantly, markerless methods avoid additional dedicated imaging (Liu et al., 2017; Mongen and Willems, 2019), thereby decreasing costs and the time required.

1.1.4. Surgery

For all surgeries, the same combined transfacial and intracranial approach was used. In order to access intracranial space and allow transfacial resection of the tumor, the authors performed a bifrontal craniotomy in tandem with transfacial exposure of the nasal cavity, ethmoid, and maxillary, and orbital areas. A more detailed description is presented in the case report section.

1.1.5. Computerized analysis of accuracy

In order to ensure the accuracy of translating virtually planned osteotomies into real resection margins, for all patients the authors segmented the postoperative CT scan data and imported both preoperative virtual planning and postoperative CT into 3-Matic software (Materialise, Leuven, BE). Alignments were coupled using a point-based registration method, which was then refined using an iterative closest point algorithm.

Part comparison analysis (PCA) was performed to provide a visual representation of differences between virtually planned and real resections. By considering preoperative CT scans as base entities and mapping virtual reality models and postoperative CT scans, differences between virtual and real craniofacial resections were highlighted in red using a threshold of 3 mm. Such maps provided a visual representation of differences between the planned and actual resections.

In order to quantitatively describe the accuracy of resection, calculation of mean error, standard deviation, and root mean square error (RMSE) was performed in all four cases. By considering a plane passing though the nasion and porion bilaterally, models were divided into intracranial and extracranial spaces, and separate measurements were accomplished for the intracranial and transfacial parts of the resection.

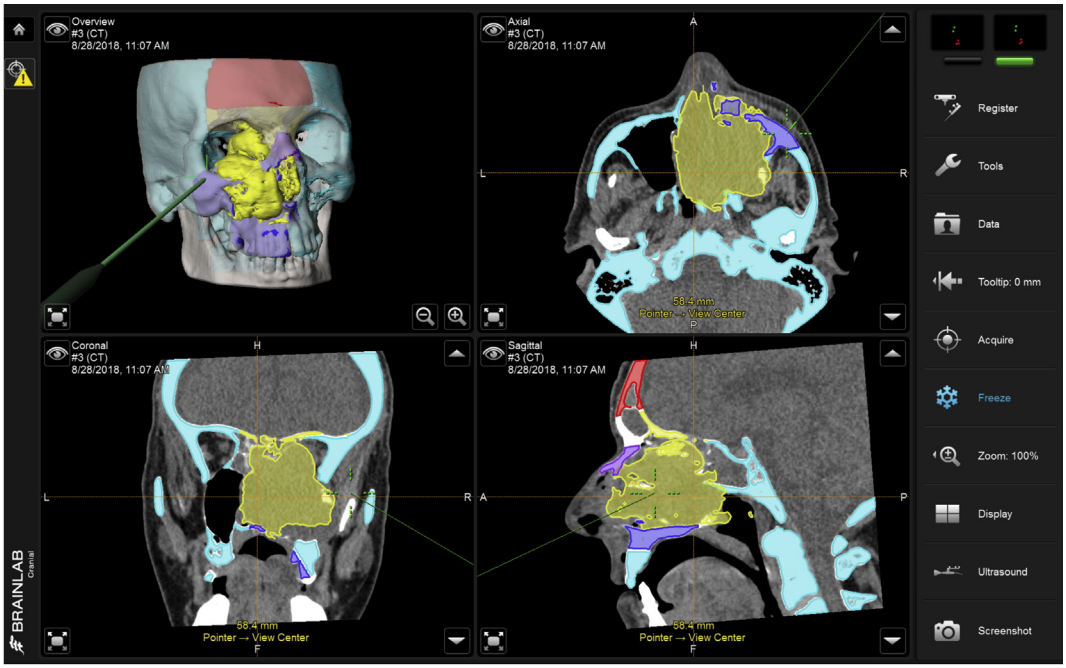

Fig. 2. Intraoperative navigation is performed on STL files exported from the personalized virtual planning process. In contrast, traditional atlas-based segmentation methods incorporated in surgical navigators do not allow navigation of a customized surgical plan, which is essential in complex craniofacial procedures. The top-left view shows three-dimensional navigation along the zygomatic resection margin.

Fig. 3 provides a comprehensive summary of the innovations introduced by our protocol, and underlines the differences between this and past or current surgical planning methods.

2. Case report

A 62-year-old male smoker presented with recurrent bleeding from the nose, progressive swelling of the right maxillary region, and right exophthalmos. The patient underwent nasal endoscopy, which showed a bleeding mass obstructing the right nasal fossa, and multiple biopsies were performed. The diagnosis was of squamous cell carcinoma of the maxillary sinus and ethmoid sinus. The patient underwent total body CT scan and contrast-enhanced CT scan, and MR for the head and neck region, according to the proposed protocol. The local extension of the tumor was staged as T4a and no distant metastases were found; the patient showed good performance status. A combined intracranial and transfacial approach was chosen to perform an anterolateral craniofacial resection. Based on the hybrid CT-MR dataset, segmentation and 3D reconstruction of bone, tumor, and critical anatomical structures were performed. Virtual surgical planning estimated the size of resection and the order of osteotomies, which were traced while considering a safety margin of at least 5 mm. The surgical navigator was set and image-to-patient registration was performed using a point pair matching algorithm based on anatomical landmarks.

Tracheostomy represented the first surgical stage. A coronal incision was performed behind the hairline. Dissection was carried down in the subgaleal layer, and attention was paid not to injure the galea, which was important for reconstructive purposes. The resulting skin flap was then elevated to the level of the supraorbital rim and frontal bone was exposed. Two bur holes were drilled bilaterally posterior to the frontozygomatic suture, and bifrontal craniotomy was conducted with a guarded craniotome through the frontal bone and anterior table of the frontal sinus to remove the frontal bone flap. Frontal lobes were mechanically retracted to gain access to the anterior cranial base. The dura was carefully incised and dissected from the anterior ventral skull base by meticulously separating the dural insertions at the crista galli, until orbital roofs, cribriform plate, and optic chiasm were exposed. No dural infiltration was observed. Piezo-navigated osteotomies were performed on the anterior skull base both anterior and posterior to the cribriform plate, according to preoperative virtual surgical planning. The anterior osteotomy was conducted through the posterior wall of frontal sinus, while the posterior osteotomy was conducted on the planum sphenoidale, anterior to the optic chiasm. The optic canal was localized in order to transect the optic nerve in its extraconal path. The superior orbital fissure and its cranial nerves were cut, along with the maxillary nerve, and the mass was displaced downwards to prepare transfacial en bloc resection of the tumor, which represented the next surgical stage.

A right-modified Weber-Ferguson incision, including upper lip split, lateral rhinotomy, and Lynch incision, was performed and the cheek flap was elevated off the maxilla, dissecting the right face until the zygomatic arch was reached. To ensure complete en bloc removal of the tumor, the authors performed resection of the surrounding structures, including orbital exenteration and total maxillectomy. This combined approach allowed transfacial en bloc resection of the tumour, which was limited superiorly by the resected anterior skull base, inferiorly and laterally by the maxilla, and medially by the nasal septum and lamina papyracea (Fig. 4).

The reconstructive phase had the primary purpose of providing effective closure of the anterior ventral skull base, thus minimizing the risk of cerebrospinal fluid (CSF) leak and preventing meningitis. Watertight closure of the dura was achieved by using a dural substitute (Duragen Secure; Integra, Plainsboro, New Jersey, USA), which was subsequently covered with a pedicled pericranial flap, thus providing a vascularized barrier separating the dura and the nasal cavity. Temporalis muscle was then rotated to provide an additional vascularized layer protecting the intracranial space. Maxillofacial reconstruction was achieved using a latissimus dorsi flap, which represents the flap of choice for reconstructing cephalic defects thanks to its long pedicle.

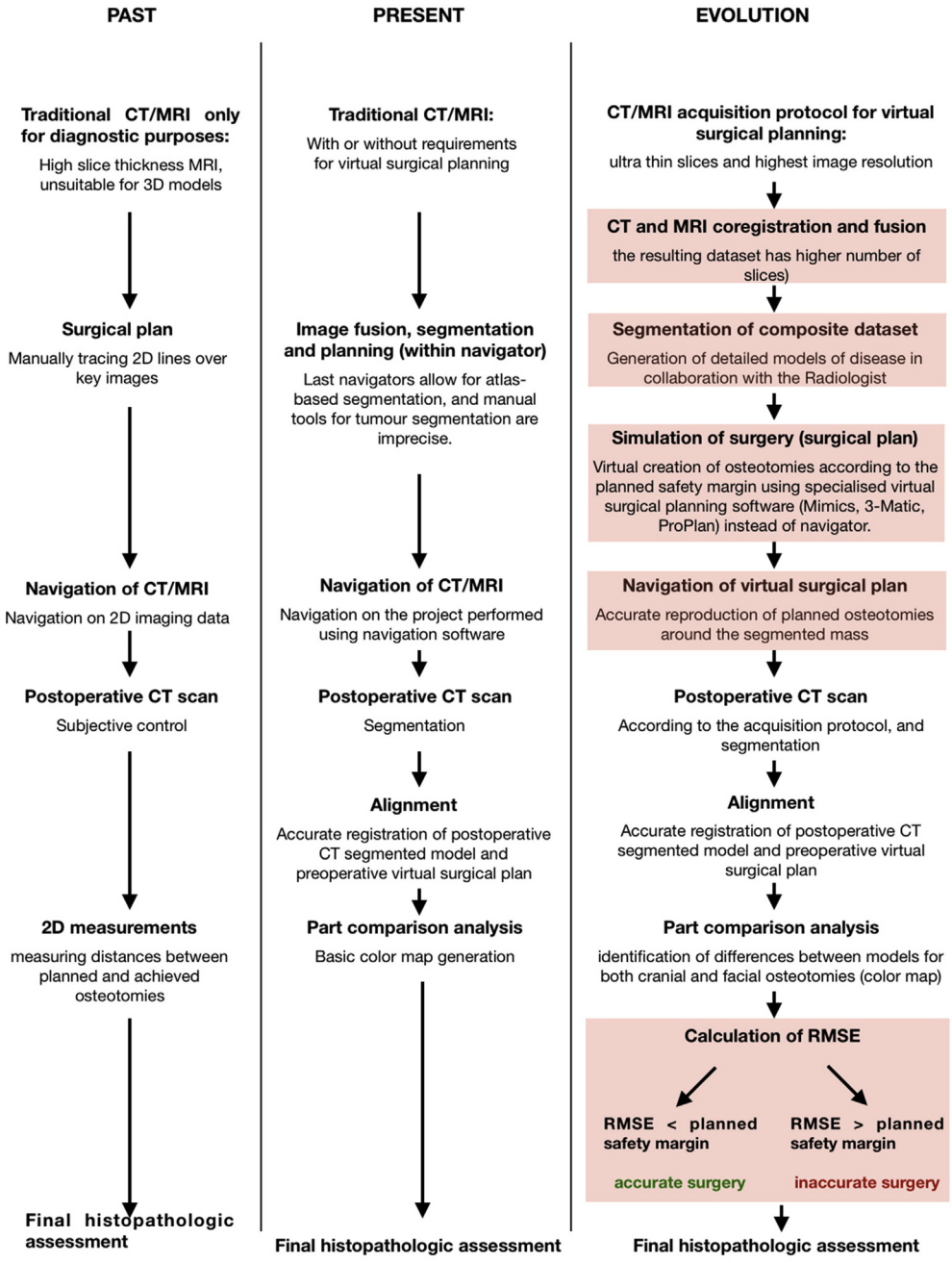

Fig. 3. Diagram showing the protocols used to manage the planning phase, navigation, and analysis of results in craniofacial resections. The evolution of the protocol is compared with previous approaches and state-of-the-art methods, and innovations are shown in red.

The operative time was 8 h and 20 min. No intraoperative or postoperative complications occurred. No cerebrospinal fluid leakage was observed.

Part comparison analysis results showed that virtual planning could be accurately reproduced in the operating room. In particular, high concordance between virtually planned and surgically performed resection was found in the anterior maxilla and zygoma. Additionally, anterior and posterior limits of intracranial osteotomies, passing through the posterior wall of the frontal sinus and planum sphenoidale, respectively, were accurately reproduced with the aid of surgical navigation (Fig. 5). Mean error, standard deviation, and root mean square error (RMSE) were determined by comparing virtual and real resections in the intracranial and transfacial parts. For the intracranial part of the resection, values were 1.086 mm for mean error, 1.132 mm for standard deviation, and 1.265 mm for RMSE. For the transfacial part of the resection, values were 1.887 mm for mean error, 1.643 mm for standard deviation, and 1.951 mm for RMSE. The volume of the resected bone was 19.571 cm^3 for the achieved resection and 18.345 cm^3 for the virtually planned resection.

Histopathological examination of resection margins was coherent with virtual analysis and found that R0 status (absence of disease) was achieved in 100% of superficial margins, 100% of deep margins, and 100% of bone margins (Table 2).

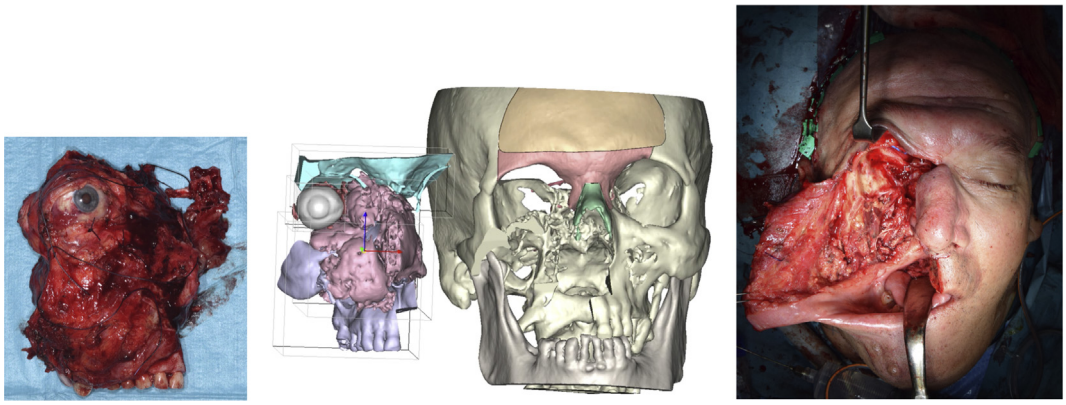

Fig. 4. Comparison between the operative field and the resected specimen using virtual surgical planning.

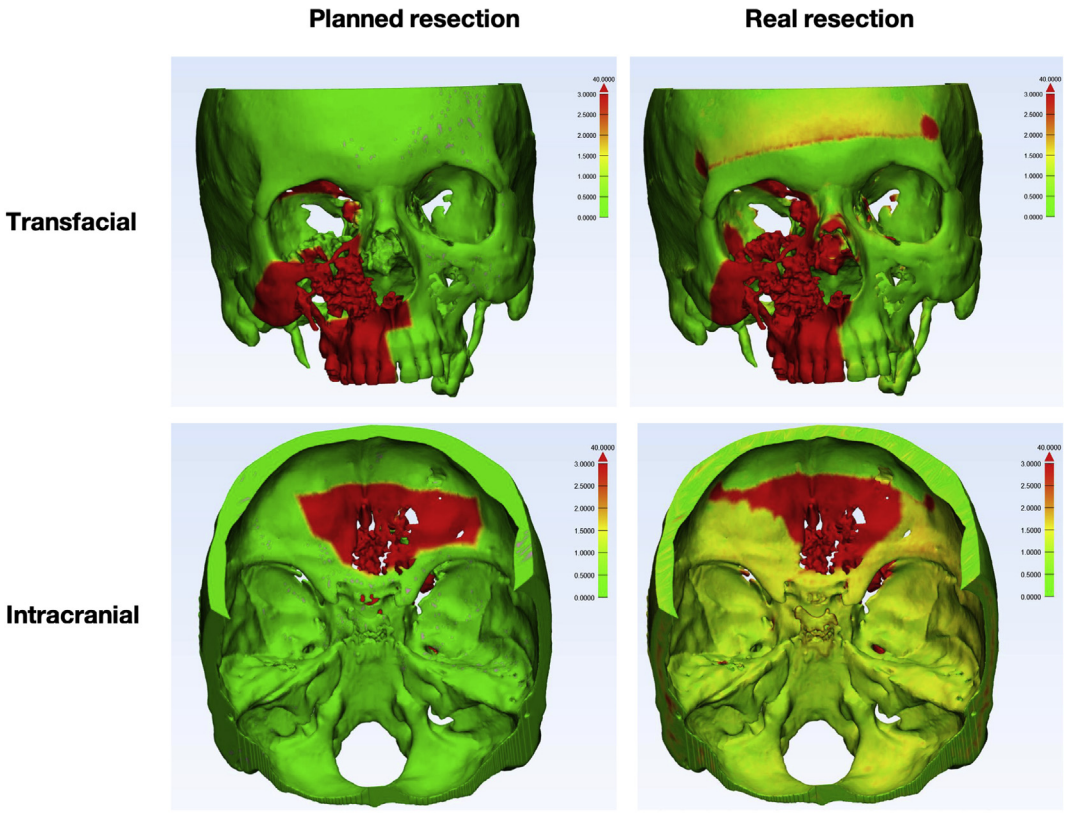

Fig. 5. Color maps generated though part comparison analysis (PCA) are useful for providing a visual comparison of resection contours between virtual surgical planning and postsurgical results. Virtual surgical planning and postoperative result are overlapped with the preoperative CT scan to generate the corresponding color map. The left column refers to the virtually planned resection, while the right column refers to the postoperatively assessed resection. The combined approach is presented as both facial and intracranial components. Results are shown with a threshold of 3 mm. Green areas indicate coincidences; red areas indicate differences.

After surgery, the patient underwent adjuvant chemotherapy based on a cisplatin regimen and radiation therapy consisting of 66 Gy given in 33 fractions to the primary tumor site and 56.1 Gy given in 33 fractions to the prophylactic nodal sites.

Fig. 6 shows the clinical and radiological outcomes after reconstruction using a latissimus dorsi flap 6 months after surgery.

3. Discussion

Oncological principles of anterior craniofacial resection remain as described by Ketcham and involve n bloc resection of tumor (Ketcham et al., 1973; Ketcham and Van Buren, 1985). In order to guarantee clean margins, it is of paramount importance that the tumor is resected within a three-dimensional volume of healthy tissue. The authors refer to the three-dimensional concept of oncological resection as 'box resection'. At the same time, care must be taken to maximize preservation of normal bony tissues and surrounding soft tissues. Many studies have investigated the importance of extending resection margins beyond the visible tumor to achieve radical resection: after a careful literature search, we planned osteotomies to include a security margin of 5 mm in order to achieve free surgical margins. It has been shown that extending

Table 2
Results evaluated in the application of computerized planning and evaluation of accuracy in examined cases.

	Surgical time (min)	Intracranial resection			Transfacial resection			Volume of resected bone (cm^3)		R status of margins (R0, R1, R2)		
		Mean error (mm)	SD (mm)	RMSE (mm)	Mean error (mm)	SD (mm)	RMSE (mm)	Virtual	Real	Superficial margins	Deep margins	Bone margins
Patient 1	520	1.158	1.179	1.652	1.235	1.229	1.742	15.189	18.712	100% R0	100% R0	100% R0
Patient 2	500	1.086	1.132	1.265	1.887	1.643	1.951	18.345	19.571	100% R0	100% R0	100% R0
Patient 3	540	1.137	1.398	1.421	1.578	1.663	1.994	13.224	14.786	100% R0	90% R0, 10% R1	100% R0
Patient 4	630	2.091	1.897	2.593	1.889	1.777	2.248	18.431	20.881	100% R0	80% R0, 20% R1	90% R0, 10% R1
	547.5	1.368	1.401	1.733	1.647	1.578	1.984	16.297	18.487	100% R0	92.5% R0	97.5% R0

Fig. 6. Postoperative situation: A) clinical; B) radiological.

resection margins from 3 mm to 5 mm can achieve improved locoregional control and survival (Amdur et al., 1989; Pfreundner et al., 2000; Langendijk et al., 2005).

In our series of patients, we performed en bloc tumor resection with an anterior craniofacial approach, removing the ethmoid cells and cribriform plate, superior nasal septum, and floor of the anterior cranial fossa, including the interorbital area in anterior craniofacial resection or a lateral extension to the orbital roof when anterolateral craniofacial resection was performed (Lund et al 1998). In cases of facial bone involvement, resection of the zygoma and maxilla was also considered.

Accurate osteotomies can ideally be traced on three-dimensional skull-base models during surgical simulation, where no blood or interposition of soft tissues occurs; however, freehand replication of osteotomies might be hazardous in a surgical setting because of the proximity of surrounding structures, such as the brain and orbit. To confirm the positional accuracy for all bone cuts, both in the facial skeleton and the skull base, a surgical navigator is recommended, which also improves the safety of craniofacial resections (Nakamura et al., 2009; Heiland et al., 2004).

In their pioneering on modern navigational surgery of the craniofacial skeleton, Schramm et al. emphasized the importance of image-guided treatment and suggested that tumor surgery is made more radical by intraoperative navigation, providing guidance over safety margins, while preserving vital structures (Schramm et al., 2000). In recent years, several studies have demonstrated that navigation can accurately reproduce planned osteotomies in the craniofacial region (Franz et al., 2018).

Traditionally, navigation has been performed on CT/MR images, which allows basic volume rendering. Surgical navigators include tools for automatic segmentation of individual structures, which generally employ atlas-based methods, where the patient is compared with a library of preexisting anatomical structures until a good match is found. Such tools allow for immediate recognition and reconstruction of anatomical parts, such as skull and face bones. However, atlas-based segmentation is impaired when there is distorted anatomy, as in cases of fracture or tumor deformation, where manual segmentation is still required (Metzger et al., 2013; Rana et al., 2012). Therefore, this study introduces the importance of navigating not only two-dimensional osteotomies, but anatomical 3D models generated from presurgical plans, providing real-time visual guidance over tumor margins and vulnerable structures, such as the internal carotid artery and optic nerve.

Although the literature describes various applications of CAD-CAM reconstruction in maxillofacial surgery, and such technology is widely applied in the field of mandibular resection and reconstruction, over recent years only a few reports have described the use of virtual surgical planning for combined transcranial and transfacial procedures. Schramm et al. identified the following indications for navigation-assisted oncological craniofacial surgery: volume assessment of the tumor before and after adjuvant therapies; trajectorially guided tumor biopsies; tumor mapping with

control over resection margins; and reconstruction after ablative tumor surgery (Schramm et al., 2000, 2006; Hohlweg-Majert et al., 2005). More recently, Tarsitano et al. investigated the role of navigation in correlating volumetric virtual planning and control of resection margins (Tarsitano et al., 2017; Ricotta et al., 2018), providing evidence that computerized planning is helpful in making surgery more radical.

However, the sequence of surgical maneuvers is difficult to simulate, due to the complex spatial arrangement of osteotomies and the sinonasal and orbital involvement of such tumors, as well as the requirement for imaging that is suitable for three-dimensional reconstruction. In particular, the literature has lacked reports describing the simulation of multiple osteotomies and selective spatial manipulation of fragments in complex digital models, as reported by Hohlweg-Majert et al. (2005) and Schramm et al. (2006). This was probably due to the wide use of volume rendering algorithms in surgical navigation, while STL model processing is better performed using modern anatomical CAD software, such as Mimics, ProPlan, and 3-Matic, which enables surgeons to trace complex spatial arrangements of osteotomies and to deal with high-resolution geometry. Therefore, our study presents a workflow combining CAD and navigation, where virtual surgical planning is performed using specialized engineering software and the resulting project is intraoperatively navigated.

The difficulty in simulating three-dimensional osteotomies explains why earliersurgical planning for craniofacial resection was performed on single CT or MRI slices by tracing two-dimensional resection lines. Such lines only have a theoretical value, and cannot be implemented with any of the current image-guided methods, such as surgical navigation. In most cases, distances were measured between a given fixed landmark and two-dimensional osteotomies, and such distances were intraoperatively reproduced when surgical navigation was performed, as reported by Nishio et al. (2017). However, there was no real navigation of osteotomies and tumor margins. Additionally, volume rendering methods used in this study were not appropriate for simulating osteotomies and performing 3D reconstruction models of tumors and vessels, for which accurate segmentation and generation of STL files is required It is also worth mentioning that not only was the use of virtual surgical planning in surgery considered, but also the usefulness of these technologies for discussing cases within multidisciplinary teams, and their importance as educational aids for maxillofacial and skull-base surgeons (Oishi et al., 2013).

In order to assess the real advantages provided by intraoperative craniofacial navigation, a comparison between virtually planned resection and postoperatively achieved result is required, but there have been few reports validating the accuracy of surgical simulation in this regard. The aforementioned study by Nishio et al. was the first attempt to provide an estimation of resection accuracy by comparing the distances between the lines of virtual resection and the lines of actual resection. However, in our opinion, two-dimensional evaluation of accuracy performed by measuring distances between planned and achieved osteotomies by matching a few anatomical landmarks is not suitable for providing feedback on the overall accuracy of the procedure. In addition, the selection of points where distances are determined is arbitrary, and greater deviation might be found in adjacent areas.

Our additional goal was to provide an overall three-dimensional assessment of the discrepancies occurring between virtually planned and surgically achieved craniofacial resection. In line with the most recent literature (Jayaratne et al., 2010; Tarsitano et al., 2018), we performed a three-dimensional accuracy analysis using part comparison analysis (PCA) to generate color maps, which provided visual feedback for the whole surface of the two aligned entities. Since facial skeleton exposure is wide and easier to access, while a surgical approach to the anterior skull base is characterized by poor visibility, we performed a separate evaluation for accuracy achieved during the neurosurgical and maxillofacial phase. Color maps showed high correspondence between the anterior and posterior borders of skull-base resection, while for maxillofacial resection the highest accuracy was found in the zygomatic and midline osteotomies, which marked the lateral and anterior limits of facial bone resection.

RMSE values were calculated from PCA. RMSE is derived from all the points making up the surface mesh (Khambay and Ullah, 2015) and therefore can be considered a more complete parameter for describing discrepancies between virtually planned and surgically achieved resections than simply calculating two-dimensional distances.

RMSE values revealed a mean excess for postoperative skull-base resection of 1.733 mm and a mean excess for postoperative facial resection of 1.984 mm, indicating that the overall accuracy was similar between maxillofacial and skull-base resection, but with the latter being more precise. This is due to the more extensive use of intraoperative navigation in the skull base to check the position of the internal carotid artery and optic nerve in relation to osteotomies. In contrast, the study by Nishio et al. reported a mean discrepancy between planned and achieved osteotomies of 3.1 mm for the inferior wall of the cavernous sinus, 3.5 mm for the inferior wall of sphenoid sinus, and 2.3 mm for the palatine bone. However, such two-dimensional distances were measured from a single point, and may have not been replicated in the same position for all patients; moreover, attention was paid to osteotomies and not to the resection itself.

Our results indicate that craniofacial resection was performed with an average error of almost 2 mm, compared with virtually planned resection, which included a minimum distance of 5 mm from the tumor, therefore confirming the macroscopic radical resection as being within the security range. A higher RMSE would increase the likelihood of non-radical resection, because the resection lines might be too close to tumor margins.

We believe that such analysis performed on 3D polygonal mesh surfaces and applied to craniofacial resection may be useful for checking if resection has been surgically appropriate, and may therefore suggest the need for adjuvant radiation therapy if RMSE approximates the security range. Moreover, the immediate availability of this analysis after postoperative CT scan, its low cost, and the possibility to visualize resected parts three-dimensionally represent additional advantages.

Our study has some limitations. It was conducted on the first four cases, and it was performed at a single institution on a small sample of patients. A real correlation between lower RMSE values and tumor-free margins might be hypothesized in this study, but further studies on larger groups of patients will be needed to validate such a concept.

Nevertheless, due to the increasing popularity of image-guided surgery and the widespread presence of modern software in hospitals, as well as the availability of engineers and designers in modern surgical teams, we hope that technological improvements introduced by this study to the complex topic of craniofacial resections will represent a valuable resource for surgeons and a real benefit for patients.

4. Conclusions

This study demonstrates how surgical planning for craniofacial resection has become more accurate with the aid of modern technology. Surgical planning has shifted towards advanced anatomical reconstruction, with the possibility of reproducing

accurate models of disease and planning osteotomies in relation to vulnerable structures. Bioengineering software provides enhanced capabilities to perform comparative analyses and gives surgeons immediate control over their work. Craniofacial resection is a complex surgical approach, which has taken advantage of modern technology at a later time than traditional maxillofacial surgical procedures. However, the benefits might be considerable.

References

Amdur RJ, Parsons JT, Mendenhall WM, Million RR, Stringer SP, Cassisi NJ: Postoperative irradiation for squamous cell carcinoma of the head and neck: an analysis of treatment results and complications. Int J Radiat Oncol Biol Phys 16: 25, 1989

Batra PS, Luong A, Kanowitz SJ, Sade B, Lee J, Lanza DC, et al: Outcomes of minimally invasive endoscopic resection of anterior skull base neoplasms. Laryngoscope 120(1): 9, 2010

Blanco AI, Chao KSC, Ozyigit G, Adli M, Thorstad WL, Simpson JR, et al: Carcinoma of paranasal sinuses: long-term outcomes with radiotherapy. Int J Radiat Oncol 59: 51, 2004

Bridger GP, Mendelsohn MS, Baldwin M, Smee R: Paranasal sinus cancer. Aust N Z J Surg 61: 290, 1991

Cantù G, Riccio S, Bimbi G, Squadrelli M, Colombo S, Compan A, et al: Craniofacial resection for malignant tumours involving the anterior skull base. Eur Arch Oto-Rhino-Laryngology 263: 647, 2006

Day KM, Gabrick KS, Sargent LA: Applications of computer technology in complex craniofacial reconstruction. Plast Reconstr Surg Glob Open 6(3): e1655, 2018

Dulguerov P, Jacobsen MS, Allal AS, Lehmann W, Calcaterra T: Nasal and paranasal sinus carcinoma: are we making progress? A series of 220 patients and a systematic review. Cancer 92(12): 3012, 2001

Eloy JA, Vivero RJ, Hoang K, Civantos FJ, Weed DT, Morcos JJ, et al: Comparison of transnasal endoscopic and open craniofacial resection for malignant tumors of the anterior skull base. Laryngoscope 119: 834, 2009

Franz L, Isola M, Bagatto D, Tuniz F, Robiony M: A novel approach to skull-base and orbital osteotomies through virtual planning and navigation. Laryngoscope 129: 823–831, 2019

Guo Y, Lopez J, Macmillan A, Cantab MA, Yang R, Dorafshar AH, et al: The use of virtual surgical planning in total facial skeletal reconstruction of Treacher Collins syndrome: a case report. Craniomaxillofac Trauma Reconstr 11(3): 230, 2018

Heiland M, Habermann CR, Schmelzle R: Indications and limitations of intraoperative navigation in maxillofacial surgery. J Oral Maxillofac Surg 62(9): 1059, 2004

Hohlweg-Majert B, Schön R, Schmelzeisen R, Gellrich NC, Schramm A: Navigational maxillofacial surgery using virtual models. World J Surg 29: 1530, 2005

Hoppe BS, Stegman LD, Zelefsky MJ, Rosenzweig KE, Wolden SL, Patel SG, et al: Treatment of nasal cavity and paranasal sinus cancer with modern radiotherapy techniques in the postoperative setting—the MSKCC experience. Int J Radiat Oncol 67: 691, 2007

Jayaratne YSN, Zwahlen RA, Lo J, Cheung LK: Three-dimensional color maps: a novel tool for assessing craniofacial changes. Surg Innov 17: 198, 2010

Ketcham AS, Chretien PB, Van Buren JM, Hoye RC, Beazley RM, Herdt JR: The ethmoid sinuses: a re-evaluation of surgical resection. Am J Surg 126: 469, 1973

Ketcham AS, Van Buren JM: Tumors of the paranasal sinuses: a therapeutic challenge. Am J Surg 150: 406, 1985

Khambay B, Ullah R: Current methods of assessing the accuracy of three-dimensional soft tissue facial predictions: technical and clinical considerations. Int J Oral Maxillofac Surg 44: 132, 2015

Langendijk JA, Slotman BJ, van derWaal I, Doornaert P, Berkof J, Leemans CR: Risk-group definition by recursive partitioning analysis of patients with squamous cell head and neck carcinoma treated with surgery and postoperative radiotherapy. Cancer 104: 1408, 2005

Liu Y, Song Z, Wang M: A new robust markerless method for automatic image-to-patient registration in image-guided neurosurgery system. Comput Assist Surg 22(1): 319, 2017

Lund VJ, Howard DJ, Wei WI, Cheesman AD: Craniofacial resection for tumors of the nasal cavity and paranasal sinuses — a 17-year experience. Head Neck 20: 97, 1998

Metzger MC, Bittermann G, Dannenberg L, Schmelzeisen R, Gellrich NC, Hohlweg-Majert B, et al: Design and development of a virtual anatomic atlas of the human skull for automatic segmentation in computer-assisted surgery, preoperative planning, and navigation. Int J Comput Assist Radiol Surg 8(5): 691, 2013

Mongen MA, Willems PWA: Current accuracy of surface matching compared to adhesive markers in patient-to-image registration. Acta Neurochirurgica 161: 865–870, 2019

Nakamura M, Sto T, Rodt T, Majdani O, Lorenz M, Lenarz T, et al: Neuronavigational guidance in craniofacial approaches for large (para)nasal tumors involving the anterior skull base and upper clival lesions 35: 666, 2009

Nishio N, Fujii M, Hayashi Y, Hiramatsu M, Maruo T: Preoperative surgical simulation and validation of the line of resection in anterolateral craniofacial resection of advanced sinonasal sinus carcinoma. Head Neck 39(3): 512, 2017

Oishi M, Fukuda M, Yajima N, Yoshida K, Takahashi M, Hiraishi T, et al: Interactive presurgical simulation applying advanced 3D imaging and modeling techniques for skull base and deep tumors. J Neurosurg 119: 94, 2013

Pfreundner L, Willner J, Marx A, Hoppe F, Beckmann G, Flentje M: The influence of the radicality of resection and dose of postoperative radiation therapy on local control and survival in carcinomas of the upper aerodigestive tract. Int J Radiat Oncol Biol Phys 47: 1287, 2000

Rana M, Essig H, Eckardt AM, Tavassol F, Ruecker M, Schramm A, et al: Advances and innovations in computer-assisted head and neck oncologic surgery. J Craniofac Surg 23: 272, 2012

Ricotta F, Cercenelli L, Battaglia S, Bortolani B, Savastio G, Marcelli E, et al: Navigation-guided resection of maxillary tumors: can a new volumetric virtual planning method improve outcomes in terms of control of resection margins? J Craniomaxillofac Surg 46(12): 2240, 2018

Robin PE, Powell DJ, Stansbie JM: Carcinoma of the nasal cavity and paranasal sinuses: incidence and presentation of different histological types. Clin Otolaryngol 4: 431, 1979

Schramm A, Gellrich NC, Gutwald R, Schipper J, Bloss H, Hustedt H, et al: Indications for computer assisted treatment of cranio-maxillofacial tumors. Comp Aided Surg 5(5): 343, 2000

Schramm A, Schoen R, Ruker M, Barth EL, Zizelmann C, Gellrich NC: Computer assisted oral and maxillofacial reconstruction. J Comput Inf Technol 14: 71, 2006

Taghi A, Ali A, Clarke P: Craniofacial resection and its role in the management of sinonasal malignancies. Expert Rev Anticancer Ther 12: 1169, 2012

Tarsitano A, Ricotta F, Baldino G, Badiali G, Pizzigallo A, Ramieri V, et al: Navigation-guided resection of maxillary tumours: the accuracy of computer-assisted surgery in terms of control of resection margins — a feasibility study. J Craniomaxillofac Surg 45(12): 2109, 2017

Tarsitano A, Battaglia S, Ricotta F, Bortolani B, Cercenelli L, Marcelli E, et al: Accuracy of CAD/CAM mandibular reconstruction: a three-dimensional, fully virtual outcome evaluation method. J Craniomaxillofac Surg 46: 1121, 2018

Turner JH, Reh DD: Incidence and survival in patients with sinonasal cancer: historical analysis of population-based data. Head Neck 34: 877, 2012

Vrionis FD, Kienstra MA, Rivera M, Padhya TA: Malignant tumors of the anterior skull base. Cancer Control 11: 144, 2004

Wang JC, Nagy L, Demke JC: Image-guided surgery and craniofacial applications: mastering the unseen. Maxillofac Plast Reconstr Surg 37(1): 43, 2015

Willems PWA, Berkelbach van der Sprenkel JW, Tulleken CAF: Comparison of adhesive markers, anatomical landmarks and surface matching in patient-to-image registration for frameless stereotaxy. Proc SPIE 4158: 156, 2001